Technetium-99m-Human Polyclonal IgG Radiolabeled via the Hydrazino Nicotinamide Derivative for Imaging Focal Sites of Infection in Rats

Michael J. Abrams, Malik Juweid, Caroline I. tenKate, David A. Schwartz, Marguerite M. Hauser, Forrest E. Gaul, Anthony J. Fuccello, Robert H. Rubin, H. William Strauss, and Alan J. Fischman

Division of Nuclear Medicine of the Department of Radiology and Infectious Disease Unit of the Medical Service, Massachusetts General Hospital and the Departments of Radiology and Medicine, Harvard Medical School, Boston, Massachusetts; Johnson Matthey Pharmaceutical Research, West Chester, Pennsylvania; and The Robert Wood Johnson Pharmaceutical Research Institute, Raritan, New Jersey

The biologic behavior of human polyclonal immunoglobulin (IgG) radiolabeled with technetium-99m (^{99m}Tc) by a novel method, via a nicotinyl hydrazine derivative, was evaluated in rats. Technetium-99m- and indium-111-IgG were co-administered to normal rats and biodistribution was determined at 2, 6, and 16 hr. The inflammation imaging properties of the two reagents were compared in rats with deep-thigh infection due to *Escherichia coli*. Blood clearance of both antibody preparations was well described by a bi-exponential function: (^{99m}Tc-IgG: $t_{½}$ = 3.82 ± 0.89 and 57.52 ± 1.70 hr, ^{111}In-IgG: 3.93 ± 0.117 and 40.71 ± 1.26 hr). Biodistributions in the solid organs were similar, however, small but statistically significant differences were detected: ^{99m}Tc-IgG > ^{111}In-IgG in lung, liver, and spleen; ^{99m}Tc-IgG < ^{111}In-IgG in kidney and skeletal muscle ($p < 0.01$). At all three imaging times, target-to-background ratio and percent residual activity for the two compounds were remarkably similar. These studies establish that human polyclonal IgG labeled with ^{99m}Tc via a nicotinyl hydrazine modified intermediate is equivalent to ^{111}In-IgG for imaging focal sites of infection in experimental animals.

J Nucl Med 1990; 31:2022–2028

Indium-111-labeled human polyclonal immunoglobulin (^{111}In-IgG) is an effective agent for imaging focal sites of inflammation in both animal models of infection and in human subjects (*1–3*). The localization of ^{111}In-IgG at sites of inflammation was originally postulated to occur by binding of the Fc portion of the molecule to specific receptors in inflammatory cells (*4*). Micro-autoradiography studies, however, revealed that there is minimal association of radiolabel with infiltrating inflammatory cells, suggesting a role for other mechanisms in localization (*5*). It appears that nonspecific protein leak into the greatly expanded protein-space of inflammatory lesions plays a significant role in the early localization of ^{111}In-IgG. Diffusion into an expanded protein space can occur rapidly, raising the possibility of early imaging for the detection of focal inflammation. The relatively small increase in volume, however, requires a very high count density image for detection. The limited photon flux of ^{111}In makes it difficult to image the early stage of this process, due to the long acquisition times required to record a sufficient count density. A technetium-99m- (^{99m}Tc) labeled radiopharmaceutical could potentially solve this problem.

In this study, we prepared ^{99m}Tc-labeled IgG by a novel method using the hydrazinonicatinamide derivative of IgG (*6*). The biodistribution and imaging properties of this preparation of IgG were compared to ^{111}In-labeled IgG.

MATERIALS AND METHODS

Radiopharmaceuticals: ^{111}In-Labeled IgG

Human polyclonal IgG (Gammimune, Cutter Laboratories, Emeryville, CA) was radiolabeled with ^{111}In (Indium Chloride, Amersham, Arlington Heights, IL) via the DTPA-carboxycarbonic anhydride chelate method as previously described (*7,8*). Typically approximately two DTPA groups were present per IgG. Radiochemical purity was determined using ITLC-sg chromatographic strips (Gelman Laboratories, Ann Arbor, MI) with 0.1 *M* sodium citrate (pH 5.5) as the solvent. All preparations had at least 90% of the radioactivity bound to antibody.

Technetium-99m-Labeled IgG

Preparation of succinimidyl 6-hydrazinopyridine-3-carboxylate hydrochloride [2,5-pyrrolidinedione, 1-[[6-hydrazino-3-

Received Mar. 1, 1990; revision accepted Jun. 6, 1990.

For reprints contact: Dr. Alan J. Fischman, Division of Nuclear Medicine, Department of Radiology, Massachusetts General Hospital, 32 Fruit St., Boston, MA 02114.

pyridinyl) carbonyl]oxy]-monohydrochloride]. The reaction sequence for the synthesis of this compound is summarized in Figure 1. 6-Chloronicotinic acid, di-tert-butyl dicarbonate and 85% hydrazine hydrate were purchased from Aldrich Chemicals (Milwaukee, WI). Dicyclohexylcarbodiimide (DCC) was purchased from Fluka Chemika (Ronkonkoma, NY). ^1H NMR spectra were obtained in DMSO-d_6 on a Bruker AF-80 spectrometer. Elemental analyses were performed at Atlantic Microlabs, Norcross, GA. The details of the synthesis are summarized in the Appendix.

Technetium-99m Labeling

The nicotinyl hydrazine derivative of human polyclonal IgG (Fig. 2) was prepared as follows: A 4 molar excess of freshly dissolved succinimidyl 6-hydrazino nicotinate hydrochloride (*4*) (30 m*M* in DMF) was added dropwise to a stirred solution of IgG (1.0 g in 20 ml of 0.1 *M* phosphate buffer, pH 7.8). The solution was stirred gently for 5 hr at room temperature protected from light. This was followed by dialysis against 10 m*M* citrate, pH 5.2 at 4°C (five buffer changes over 24 hr). The mixture was then filtered through a 0.2-μm filter and protein concentration was determined by the Bradford method (*9*). The solution was diluted to 5 mg/ml with buffer (100 m*M* NaCl, 20 m*M* citrate, 1% mannitol, pH 5.2), divided into 200 μl aliquots and stored frozen at −20°C. The number of hydrazino groups introduced was determined by converting the hydrazino groups to the corresponding hydrazone by reaction with p-nitrobenzaldehyde and measuring the optical density at 385 nm (extinction coefficient: 2.53×10^4 L·mol^{-1}·cm^{-1}). Typically, approximately three nicotinyl hydrazine groups were present per IgG.

The nicotinyl hydrazine modified IgG was radiolabeled with ^{99m}Tc by reaction with ^{99m}Tc-glucoheptonate, which was freshly prepared with a standard kit (Squibb, Princeton, NJ). Twenty millicuries of ^{99m}Tc-glucoheptonate was added to 0.5 ml of a solution of nicotinyl hydrazine modified IgG (5.0 mg/ml in citrate buffer, pH = 5.2) and the mixture was incubated for 60 min at room temperature. Radiochemical purity was determined using ITLC-sg chromatographic strips (Gelman Laboratories Ann Arbor, MI) with 0.1 *M* sodium citrate (pH 5.5) as the solvent. All preparations had at least 90% of the radioactivity bound to antibody.

In a control experiment, the antibody was subjected to the same derivatization and labeling procedures as described above with the exception that 6-hydrazino nicotinate hydrochloride was substituted for succinimidyl 6-hydrazino nicotinate hydrochloride. Under these circumstances, only 6% of the radioactivity was associated with protein.

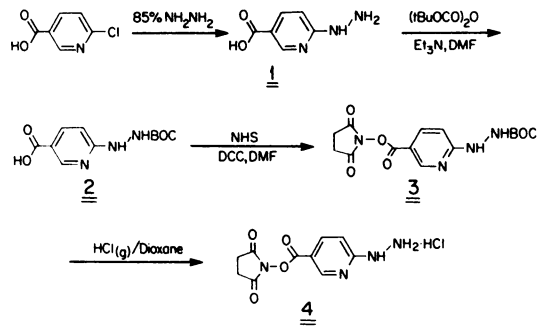

FIGURE 1
Reaction sequence for the preparation of succinimidyl 6-hydrazinopyridine-3-carboxylate hydrochloride.

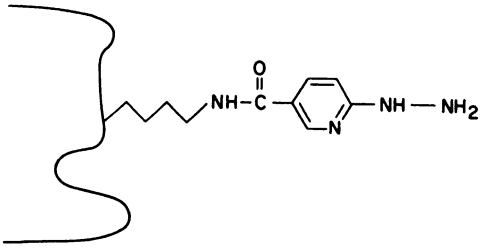

FIGURE 2
Schematic diagram of a hydrazino nicatinamide derivative of human polyclonal IgG. In the radiolabeling reaction, the hydrazine group reacts with ^{99m}Tc-glucoheptonate, possibly forming a ^{99m}Tc-diazenido linkage.

Stability of ^{99m}Tc-IgG

Technetium-99m-labeled IgG was incubated at 37°C with an equal volume of pooled human serum. After 2.5 and 5.5 hr of incubation, aliquots of the reaction mixture were diluted 1:5 with phosphate-buffered saline (pH 7.4) and analyzed by ITLC and high-performance liquid chromatography (HPLC). For HPLC, the samples were applied to a TSK 3000 column (60 × 2.5 cm) eluted with 20 m*M* citrate/100 m*M* NaCl, pH 6.0, flow rate 1.0 ml/min. The column was monitored by ultraviolet absorption (OD_{280}) and radioactivity measurement. In another experiment, ^{99m}Tc-labeled IgG was incubated at 37°C with human serum for 75 min and the reaction mixture was analyzed by SDS-PAGE (12.5% gel).

Animal Model

A single clinical isolate of *Escherichia coli* was employed to produce focal infection. The bacteria were incubated overnight on trypticase soy agar plates at 37°C, and individual colonies were diluted with sterile normal saline to produce a turbid suspension containing approximately 2×10^9 organisms/ml. Male Sprague-Dawley rats, weighing ~150 g (Charles River Breeding Laboratories, Burlington, MA) were anesthetized with ketamine and 0.1 ml of a suspension of bacteria was injected into the left posterior thigh (*11*). A range of infection intensities was produced for the imaging studies by varying the number of organisms from 5×10^7 to 2×10^8.

Imaging

Twenty-four hours after bacterial inoculation, when gross swelling was apparent in the thigh, a mixture of the radiolabeled proteins (~0.25 mg/kg of each protein derivative labeled with 100–150 μCi of ^{111}In or 1.0 mCi of ^{99m}Tc) was injected intravenously via the tail vein. Following injection of the radiolabeled reagents, whole-body scintigrams of ketamine anesthetized animals were acquired using a large field of view scintillation camera equipped with a parallel-hole medium-energy collimator interfaced to a dedicated computer system (Technicare 438, Technicare 560, Solon, Ohio). Images were recorded for a preset time of 10 min/view. Indium-111 and ^{99m}Tc images were acquired sequentially with 15% windows centered on photopeaks at 140 keV for ^{99m}Tc and 247 keV for ^{111}In. By imaging animals that were injected with only ^{111}In-IgG in the ^{99m}Tc window, the amount of crossover of the 174 keV photons of ^{111}In into the ^{99m}Tc window was deter-

mined. This factor was used to correct all images acquired after dual-isotope injection.

Regions of interest were drawn around the infected area, a similar area in the contralateral thigh, and the whole animal to calculate target-to-background (T/B) ratio (infected thigh/contralateral high) and percent residual activity (%RA in infected thigh/whole animal). At the conclusion of imaging, the animals were killed with ether anesthesia, autopsied, and the site of infection was cultured.

Biodistribution

To compare the in-vivo behavior of the ^{99m}Tc-labeled IgG to that of ^{111}In-IgG, biodistribution studies were performed in 18 normal (uninfected) rats. The animals were simultaneously injected with 10 μCi of ^{99m}Tc-IgG and 2 μCi of ^{111}In-IgG to determine the biodistribution at 2, 6, and 16 hr after injection (each protein was evaluated in six animals at each time point). An aliquot of the injected dose and samples of blood, heart, lung, livers, spleen, kidney, muscle, testis, and intestine were weighed and counted in a well-type gamma counter (LKB model #1282, Wallac Oy, Finland). The results were expressed as percent injected dose per gram and percent injected dose per organ. For blood and muscle, percent injected dose per organ was calculated as previously described (*10*).

In another experiment, more detailed data on the blood clearance of ^{99m}Tc- and ^{111}In-labeled IgG were obtained. In this experiment, a group of five normal rats was simultaneously injected with 3.0 mCi of ^{99m}Tc-IgG and 6.0 μCi of ^{111}In-IgG and serial blood samples were collected at 1, 3, 6, 21, 27, 33, 46, and 51 hr.

Statistical Methods

The results of the biodistribution studies were evaluated by analysis of variance followed by Duncan's new multiple range test (*11*). Kinetic parameters for blood parameters were derived by non-linear regression analysis using a biexponential model. The results of the imaging studies were analyzed by linear regression. All results are expressed as mean ± s.e.m.

RESULTS

Radiolabeling

Nicotinyl hydrazine modified IgG is readily radiolabeled with ^{99m}Tc by reaction with ^{99m}Tc-glucoheptonate. Radiochemical purity determined by ITLC was at least 90% (typically > 95%). Based on control experiments in which the 6-hydrazino nicotinate hydrochloride was substituted for succinimidyl 6-hydrazino nicotinate hydrochloride in the protein derivatization procedure, it is clear that ^{99m}Tc binding is highly specific (only 6% of added radioactivity was associated with protein).

HPLC profiles of ^{99m}Tc-labeled IgG incubated with human serum for 2.5 and 5.5 hr demonstrated that at both times, nearly all of the radioactivity was associated with the IgG fraction with no apparent labeling of other plasma proteins. ITLC showed that at 5.5 hr only 5% of the radioactivity was present as low molecular weight species. SDS-PAGE of ^{99m}Tc-labeled IgG incubated at 37°C with human serum for 75 min showed that 93% of the radioactivity migrated in the molecular weight region corresponding to IgG. Less than 2% of the radioactivity was detected in the stacking gel, indicating that the amount of radiolabeled colloid was minimal.

Imaging

The animals tolerated the i.v. administration of both ^{111}In- and ^{99m}Tc-labeled IgG without apparent ill effects. Both preparations showed definite localization at the site of infection at 3–5, 12–15, and 24 hr after injection. With both agents, the greatest accumulation occurred at 24 hr (Fig. 3). As is readily apparent in Figure 4 and Table 1, at the earliest time point the T/B ratio and %RA were nearly identical with the two radiopharmaceuticals. At the intermediate time point, the images acquired with indium-labeled IgG had slightly (not statistically significant) higher T/B ratios and %RAs. At the latest time point, this difference increased slightly and reached statistical significance.

Biodistribution

Both antibody preparations showed a monotonic decrease in blood concentration over time (Fig. 5). The clearance curves were well described by a bi-exponential function ($r^2 > 0.95$). The derived kinetic parameters are summarized in Table 2. The first component of clearance was not significantly different for the two preparations, however, the second component was significantly slower ($p < 0.01$) with the ^{99m}Tc-labeled antibody ($t_{½}$: 57.52 ± 1.70 versus 40.71 ± 1.26 hr).

The biodistribution in solid organs is shown in Figure 6. In general, the biodistribution of the two preparations were remarkably similar at all time points. However, several small but statistically significant differences were detected. In lung, liver, and spleen, ^{99m}Tc-IgG accumulated to a greater extent than ^{111}In-IgG ($p < 0.01$), while in kidney and muscle, the reverse was true. In the heart, the gastrointestinal tract, and testis, no significant differences in accumulation were observed.

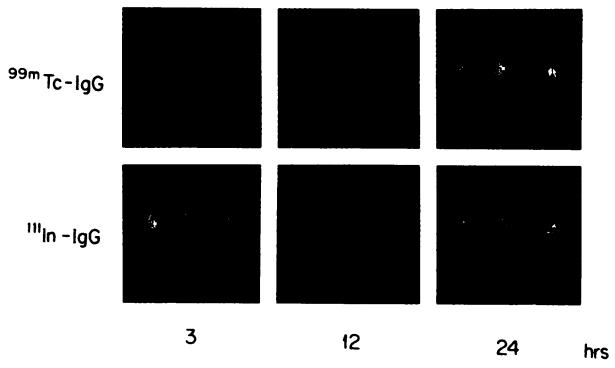

FIGURE 3
Gamma camera images of a group of rats with *E. coli* deep-thigh infections at 2, 12, and 24 hr after injection of ^{99m}Tc- and ^{111}In-labeled human polyclonal IgG. Infections were established 24 hr prior to injection. These images represent a subset of the data presented in Figure 4.

TABLE 1
Regression Parameters for T/B Ratio and %RA in Rats with Deep-Thigh *E. Coli* Infection Injected with ^{99m}Tc- and ^{111}In-Labeled IgG

	T/B Ratio			%RA		
Time*	Slope†	Intercept†	r‡§	Slope†	Intercept†	r‡§
3–5	0.99	0.12	0.89	0.93	0.20	0.86
	(0.10)	(0.19)	(0.40)	(0.11)	(0.19)	(0.59)
12–15	0.98	0.048	0.95	0.98	0.23	0.94
	(0.051)	(0.092)	(0.16)	(0.058)	(0.14)	(0.40)
24	0.89	0.40¶	0.94	0.92	0.63¶	0.97
	(0.057)	(0.15)	(0.35)	(0.36)	(0.13)	(0.38)

* Time after injection (hours). Animals were injected 24 hr after infection.
† Number in parenthesis is the standard error.
‡ Number in parenthesis is the s.e.e.
§ $p < 0.001$.
¶ $p < 0.05$.

DISCUSSION

Radiolabeled human polyclonal IgG readily accumulates in inflammatory lesions to an extent sufficient to yield excellent external images. This report compares ^{99m}Tc-IgG to ^{111}In-IgG. The radiopharmaceuticals have very similar imaging and biodistribution properties. Although the indium-labeled antibody has slightly better targeting properties at the later time points, the difference will probably not be of clinical significance. The observation that ^{99m}Tc-IgG has slightly greater accumulation in normal liver and spleen should not pose a problem in the clinical application of this reagent, since the high level of accumulation of even ^{111}In-IgG has made the evaluation of focal sites of infection nearly impossible in these areas. The reason for this greater accumulation is uncertain since, based on the in vitro studies presented here, it is clear that significant amounts of ^{99m}Tc-labeled colloids are not produced. The higher level of accumulation of ^{99m}Tc-IgG in normal lung is a potential disadvantage of the agent, since delayed imaging (>24 hr after injection) with ^{111}In-IgG has been an effective means of identifying pulmonary infections. In contrast, the lower level of accumulation of ^{99m}Tc-IgG in normal muscle may prove to be an advantage for the identification of soft-tissue inflammation.

Other methods that have been used to label antibodies with technetium include: direct binding of technetium to donor atoms on the protein, bifunctional chelating agents, and conjugation of a preformed ^{99m}Tc-4,5-bis(thioacetanido)pentanoate active ester to protein amine groups (N_2S_2-method) (*12*). While all of these techniques have been successfully applied in specific situations, significant limitations exist. With the direct method, there is marked dispersion in the affinity of donor sites on the protein for technetium, which results in significant dissociation of the technetium-antibody complex with time. Also, with some of the methods used to reduce pertechnetate, significant amounts of antibody-associated radiolabeled colloid can be formed, which results in elevated accumulation of radiolabel in elements of the reticuloendothelial system. The bifunctional chelate method suffers from the problems of:

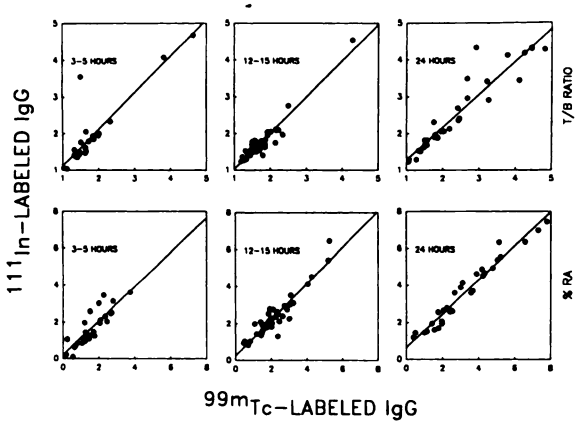

FIGURE 4
Target-to-background ratio (A) and %RA (B) of sites of infection in rats with *E. coli* deep-thigh infections imaged at 3–5 hr (n = 28), 12–15 hr (n = 43), and 24 hr (n = 32) after injection of ^{99m}Tc- and ^{111}In-labeled human polyclonal IgG. In all cases, the animals were infected 24 hr prior to injection.

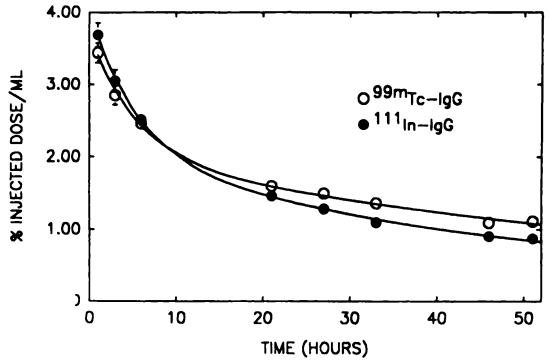

FIGURE 5
Blood clearance curves of ^{99m}Tc- and ^{111}In-labeled human polyclonal IgG. Each point is the mean ± s.e.m. for five animals.

TABLE 2
Kinetic Parameters for Blood Clearance of ^{99m}Tc- and ^{111}In-Labeled IgG

	A^1*	$t^1_{½}$ (hr)	A^2	$t^2_{½}$ (hr)	r^2
^{99m}Tc-IgG	1.71 ± 0.23†	3.82 ± 0.09	2.00 ± 0.23	57.52 ± 1.70	0.96
^{111}In-IgG	2.04 ± 0.32	3.93 ± 0.12	2.00 ± 0.34	40.71 ± 1.26	0.97

* The clearance data were fit to the equation:

$$\text{Activity} = A^1 * \exp(-0.693t/t^1_{½}) + A^2 * \exp(-0.693t/t^2_{½}).$$

† Mean ± standard error.

adventitious binding of technetium to the antibody, formation and binding of colloids to antibody, and low yield of specifically bound technetium (*13*).

Some of the problems inherent to the direct and bifunctional chelate, diethylenetriaminepentaacetic acid (DTPA), methods have been elegantly illustrated in a previous study in which the biodistribution of an antibody radiolabeled by these methods was comparable to the ^{111}In-labeled DTPA conjugate (*13*). At 1 hr after injection, there was good agreement between the biodistributions of the ^{111}In- and ^{99m}Tc-labeled DTPA coupled antibodies; while with the directly labeled antibody, there was much greater accumulation of radioactivity in liver and spleen. At 20 hr after injection, there was marked divergence between the distributions of the ^{111}In- and ^{99m}Tc-labeled DTPA coupled antibodies. These results indicate that the in vivo stability of ^{99m}Tc-labeled DTPA coupled antibody is greater than directly labeled antibody but less than ^{111}In-labeled DTPA coupled antibody. Also, the clearance half-time of the ^{99m}Tc-labeled DTPA coupled antibody was greater than the directly labeled antibody but less than the ^{111}In-labeled DTPA coupled antibody, suggesting that there may have been a higher level of protein degradation in the ^{99m}Tc-labeled antibody preparations.

In the present study, we demonstrated that ^{99m}Tc-hydrazino nicatinamide IgG has high in vitro stability in serum. The marked similarity of the biodistributions of ^{99m}Tc-IgG and ^{111}In-IgG suggests that the radiopharmaceuticals have very similar in vivo stability. In addition, the observation that the rate of blood clearance of ^{99m}Tc-IgG is slower than ^{111}In-IgG suggests that protein integrity is well maintained with the hydrazinonicotinamide labeling approach. Antibodies radiolabeled by the N_2S_2 method also have high in vivo stability, however, the labeling methodology is much more complicated than the hydrazino-nicotinamide method.

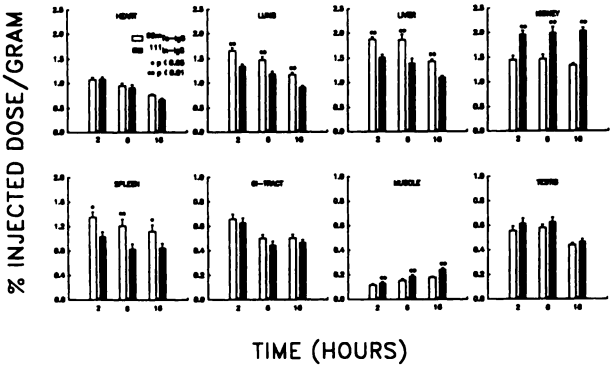

FIGURE 6
Biodistribution of ^{99m}Tc- and ^{111}In-labeled human polyclonal IgG in uninfected animals expressed as percent injected dose/gram. Each point is the mean ± s.e.m. for six animals.

Our experience with ^{111}In-IgG for imaging focal sites of inflammation in human subjects has demonstrated that most lesions can be detected within 24 hr after injection (*1,3*). This data suggests that ^{99m}Tc-IgG should be an equally effective imaging agent. Based on the biodistribution data, preliminary MIRDOSE calculations indicate that ~20 mCi of ^{99m}Tc-IgG could be administered without delivering a radiation burden in excess of 2 rads to any organ (unpublished results). Based on the physical properties of ^{111}In and ^{99m}Tc, nearly three-fold greater photon fluxes should be present at the lesion site 18 hr postinjection if ten-fold more ^{99m}Tc-IgG is injected initially. In addition, due to the intrinsically better imaging properties of ^{99m}Tc and the greater photon fluxes at early time points (10.33 mCi at 6 hr after injection of 20 mCi of ^{99m}Tc-IgG versus 1.88 mCi for 2.0 mCi of ^{111}In-IgG), the technetium-labeled protein will provide a much better signal for early detection of increased protein space at sites of inflammation. If data are recorded with SPECT, lesions may be more readily detectable with the technetium-labeled antibody at earlier times after injection. The only case in which the indium-labeled reagent will be clearly superior is the situation in which lesions are only apparent at significantly greater than 24 hr post-injection. To date, these cases have been rare except in subjects with suspected infection of vascular grafts (*14*).

In conclusion, the results of this study establish that ^{99m}Tc-IgG labeled via the hydrazino nicatinamide intermediate is equivalent to ^{111}In-IgG for imaging focal sites of infection in experimental animals. The greater general availability and superior imaging properties of ^{99m}Tc may ultimately make this radiopharmaceutical the reagent of choice for inflammation imaging in many clinical situations.

ACKNOWLEDGMENTS

This study was supported in part by grants from the Robert Wood Johnson Pharmaceutical Research Institute, Raritan, NJ, the Edw. Mallinkrodt, Jr. Foundation, St. Louis, MO, and the DOE, grants DE-F602-86 ER60460.

APPENDIX

Synthesis of succinimidyl 6-hydrazinopyridine-3-carboxylate hydrochloride [2,5-pyrrolidinedione, 1-[[6-hydrazino-3-pyridinyl) carbonyl]oxy]-monohydrochloride].

Compound reference numbers refer to Figure 1.

6-Hydrazinopyridine-3-carboxylic acid (1). 6-Chloronicotinic acid (8.0 g; 50.77 mmol) was added to 80% hydrazine hydrate (35 ml; 930.0 mmol) and placed in a 100°C oil bath for 4 hr. The homogeneous reaction mixture was cooled to room temperature and concentrated to dryness to give a white solid. The solid was dissolved in water and on acidification to pH 5.5 with concentrated hydrochloric acid a precipitate was formed. The precipitate was isolated by filtration and the solid was washed with 95% ethanol and ether and dried in vacuo to give 6.0 g of 6-hydrazinopyridine-3-carboxylic acid; yield 77%; m.p. 292–293°C; ^{1}H NMRδ: 6.69 (d, J = 8 Hz, 1 H), 7.84 (dd, J = 2.4, 8.8 Hz, 1 H), 8.51 (d, J = 2.4 Hz, 1 H). Analysis: calculated for $C_6H_7N_3O_2$: C, 47.06; H, 4.61; N, 27.44. Found: C, 46.74, H, 4.38; N, 27.27.

6-BOC-hydrazinopyridine-3-carboxylic acid (2). To a solution of 6-hydrazinopyridine-3-carboxylic acid (*1*) (1.4 g; 9.8 mmol) and triethyl amine (1.2 ml; 11.8 mmol) in DMF (10 ml) was added di-tert-buty dicarbonate (2.13 g; 9.8 mmol). The reaction mixture became homogeneous over 1 hr and stirring was continued for 16 hr at room temperature. The reaction mixture was concentrated to dryness under reduced pressure to give a brown solid. The residue was dissolved in a minimum amount of ethyl acetate and passed through silica gel 60 (230–400 mesh) using ethyl acetate as eluant to remove colored impurities. The eluate was concentrated to dryness to give the desired product, which was used without further purification; yield 2.33 g (94%). ^{1}H NMRδ: 1.40 (s, 9 H), 6.52 (d, J = 8.8 Hz, 1 H), 7.97 (dd, J = 2.4, 8.8 Hz, 1 H), 8.58 (d, J = 2.4, 1 H).

Succinimidyl 6-BOC-hydrazinopyridine-3-carboxylic acid (3). To a solution of 6-BOC-hydrazinopyridine-3-carboxylic acid (*2*) (1.45 g; 5.75 mmol) and N-hydroxysuccinimide (0.66 g; 5.75 mmol) in DMF (15 ml) was added a solution of dicyclohexylcarbodiimide (1.18 g; 5.75 mmol) in DMF (5 ml). The reaction mixture became cloudy after 1 hr and stirring was continued for 16 hr at room temperature. The reaction mixture was filtered and the filtrate was concentrated to dryness to give a brown residue. The residue was dissolved in a minimum amount of ethyl acetate and passed through silica gel 60 (230–400 mesh) using ethyl acetate as an eluant. The eluate was concentrated to dryness to give 1.2 g of a yellow solid, which was recrystallized from ethyl acetate/hexanes; yield 60%; m.p. 169.5–172°C; ^{1}H NMRδ: 1.41 (s, 9 H), 2.87 (s, 4 H), 6.64 (d, J = 8.8 Hz, 1 H), 8.08 (dd, 2.4, 8.8 Hz, 1 H), 8.73 (d, J = 2.4 Hz, 1H). Analysis: calculated for $C_{15}H_{18}N_4O_4$: C, 51.43; H, 5.18; N, 15.99. Found: C, 51.81; H, 5.26; N, 15.60.

Succinimidyl-6-hydrazinopyridine-3-carboxylic acid (4). A solution of HCl in dioxane was prepared by bubbling HCl into dioxane (20 ml) at a moderate rate for 10 min. Succinimidyl 6-BOC-hydrazinopyridine-3-carboxylic acid (*3*) (100 mg; 0.285 mmol) was dissolved in dioxane (2 ml), HCl/dioxane (2 ml) was added, and the reaction mixture was stirred at room temperature. After 5 min, the solution became cloudy and a precipitate formed. Stirring was continued for 4 hr. The cloudy reaction mixture was filtered and the solids were washed repeatedly with ether to give 55 mg of a white solid; yield 67%. ^{1}H NMRδ: 2.88 (s, 9H), 7.01 (d, J = 8.8 Hz, 1H), 8.19 (dd, J = 2.4 Hz, 1H), 8.83 (d, 8.8 Hz, 1H). Analysis: calculated for $C_{10}H_{11}ClN_4O_4$: C, 41.87%; H, 3.87%; Cl, 12.37; N, 19.53. Found: C, 41.92%; H, 3.90%; Cl, 12.30; N, 19.47.

REFERENCES

1. Fischman AJ, Rubin RH, Khaw BA, et al. Detection of acute inflammation with ^{111}In-labeled non-specific polyclonal IgG. *Semin Nucl Med* 1988; 18:335–344.
2. Rubin RH, Fischman AJ, Nedelman M, et al. The use of radiolabeled, nonspecific polyclonal human immunoglobulin in the detection of focal inflammation by scintigraphy: comparison with gallium-67-citrate and technetium-99m-labeled albumin. *J Nucl Med* 1989; 30:385–389.
3. Rubin RH, Fischman AJ, Callahan RJ, et al. ^{111}In-labeled nonspecific immunoglobulin scanning in the detection of focal infection. *N Engl J Med* 1989; 321:935–940.
4. Fischman AJ, Wilkinson R, Khaw BA, et al. Imaging of localized bacterial infections with radiolabeled nonspecific antibody fragments [Abstract]. *J Nucl Med* 1988; 29:P887.
5. Morrell EM, Tompkins RG, Fischman AJ, et al. An autoradiographic method for quantitation of radiolabeled proteins in tissue using indium-111. *J Nucl Med* 1989; 30:1538–1545.
6. Abrams MJ, Schwartz DA, Hauser MM, et al. A novel method of labeling proteins with technetium-99m based on bifunctional aromatic hydrazines [Abstract]. *J Nucl Med* 1990; 31:P776.
7. Krejcarek GE, Tucker KL. Covalent attachment of chelating groups to macromolecules. *Biochem Biophys Res Comm* 1977; 77:581–585.
8. Khaw BA, Mattis JA, Melincoff G, et al. Imaging of experimental myocardial infarction. *Hybridoma* 1984; 3:11–23.
9. Bradford MM. A rapid and sensitive method for the quantitation of microgram quantities of protein utilizing the principle of protein-dye binding. *Anal Biochem* 1976; 72:248–254.
10. Baker HC, Lindsey RJ, Weisbroth SH. *The laboratory rat.*

New York: Academic Press; 1980:257.
11. Duncan DB. Multiple range tests and multiple F-tests. *Biometrics* 1955; 11:1–42.
12. Fritzberg AR, Abrams PL, Beaumier PL, et al. Specific and stable labeling of antibodies with technetium-99m with a diamide dithiolate chelating agent. *Proc Natl Acad Sci USA* 1988; 85:4025–4029.
13. Childs RL, Hnatowich DJ. Optimum conditions for labeling of DTPA-coupled antibodies with technetium-99m. *J Nucl Med* 1985; 26:293–299.
14. LaMuraglia GM, Fischman AJ, Strauss HW, et al. Utility of the indium-111-labeled human immunoglobulin G scan for the detection of focal vascular graft infection. *J Vasc Surg* 1989; 10:20–27.

SELF-STUDY TEST
Skeletal Nuclear Medicine

ANSWERS

(continued from p. 2010)

ITEM 1: Techniques of Bone Mineral Measurement

ANSWERS: **A:** *T;* **B:** *F;* **C:** *F;* **D:** *T*

With quantitative computed tomography (QCT), trabecular bone is measured in the vertebral body. The results are expressed as milligrams of bone per cubic millimeter. With this technique, measured rates of bone loss after menopause are higher than those measured by dual-photon absorptiometry (DPA) in the entire vertebra. When the entire vertebra is measured by QCT, however, the results with DPA and QCT are quite comparable.

The varying composition of the skeleton with respect to cortical and trabecular bone and differential effects of diseases on different parts of the skeleton are the reasons that measurements from different bone sites are not interchangeable. In the midradius, 95% of bone is cortical bone. Several studies have shown that trabecular bone sites, such as the spine or distal radius, show more pronounced and earlier loss than the midradius.

Recent attention has centered on the most distal part of the radius and the calcaneus, where the proportions of trabecular bone are similar (about 60% of total bone) to that in the spine. Whether or not it is possible to predict spinal or femoral neck bone mineral density from these measurements with sufficient reliability for decision making in patient management remains controversial.

Radiation dose with one measurement on the spine is below 10 mrads for DPA, but between 0.3 and 1.0 rad for QCT.

References

1. Genant HK, Block JE, Steiger P, Glueer C-C, Smith R. Quantitative computed tomography in assessment of osteoporosis. *Semin Nucl Med* 1987;17:316–333.
2. Wahner HW. Single- and dual-photon absorptiometry in osteoporosis and osteomalacia. *Semin Nucl Med* 1987;17:305–315.

ITEM 2: Ischemic Necrosis of Bone

ANSWERS: **A:** *F;* **B:** *T;* **C:** *F;* **D:** *F;* **E:** *F*

Bone infarcts occur commonly in lupus erythematosus, whether or not the patient is under steroid treatment, but the ends of bones (rather than the diaphyses) are the usual sites of infarction and of associated abnormalities on bone marrow scintigraphy with ^{99m}Tc-colloids. In contrast, diaphyseal infarcts are common in patients with sickle cell disease.

A major drawback of ^{99m}Tc-colloid scintigraphy for the detection of ischemic necrosis of femoral heads in adults is that the uptake of this reticuloendothelial tracer diminishes progressively with age, although usually in a symmetrical fashion. This normally decreased uptake of ^{99m}Tc-colloid in older patients makes it difficult to determine if there is ischemic injury to the bone marrow. Consequently, imaging with ^{99m}Tc-MDP, the uptake of which is dependent on the integrity of the vascular supply, is more reliable in disclosing both the photopenic lesions of early avascular necrosis of the femoral head and the increased activity associated with more advanced stages of the disorder.

As noted above, the first manifestation of bone infarction with ^{99m}Tc-MDP scintigraphy is focally decreased activity, reflecting the reduced delivery of tracer to the lesion. During the revascularization phase, focally increased activity is noted, and this, obviously, is a much less specific finding. When both infarction and osteomyelitis are reasonable explanations for the patient's symptoms, as is frequently the case in sickle cell anemia, bone scintigraphy alone generally is inadequate for differentiation. With both entities, the uptake of ^{99m}Tc-MDP may be either decreased (albeit an uncommon appearance of osteomyelitis) or increased. Further evaluation by ^{67}Ga scintigraphy assists in the differential diagnosis. Osetomyelitis is likely when the uptake of ^{67}Ga in the lesion is more intense (relative to normal bone) than the uptake of ^{99m}Tc-MDP or when the spatial distribution of the two tracers is incongruent. A congruent distribution of the tracers of equivalent, moderate intensity is an indeterminate finding, although it more often indicates healing infarction than active infection.

References

1. Amundsen TR, Siegel MJ, Siegel BA. Osteomyelitis and infarction in sickle cell hemoglobinopathies: differentation by combined technetium and gallium scintigraphy. *Radiology* 1984;153:807–812.
2. Armas RR, Goldsmith SJ. Gallium scintigraphy in bone infarction. Correlation with bone imaging. *Clin Nucl Med* 1984;9:1–3.
3. Datz FL, Taylor A Jr. The clinical use of radionuclide bone marrow imaging. *Semin Nucl Med* 1985;15:239–259.
4. Williams AG, Mettler FA Jr. Christie JH. Sulfur colloid distribution in normal hips. *Clin Nucl Med* 1983;8:490–492.

ITEM 3: Scintigraphy in Acute Rheumatoid Synovitis

ANSWERS: **A:** *F;* **B:** *F;* **C:** *T;* **D:** *F;* **E:** *T;* **F:** *F*

Many different radiopharmaceuticals, including ^{99m}Tc-phosphates, ^{99m}Tc-pertechnetate, ^{67}Ga-citrate, and ^{111}In-leukocytes, have been employed to evaluate the distribution and level of disease activity in rheumatoid arthritis and other synovial inflammatory diseases. Although these different approaches often provide comparable information, important differences in the biodistribution of these agents influence the scintigraphic patterns observed.

Joint scintigraphy with ^{99m}Tc-pertechnetate demonstrates the hyperemia and increased capillary permeability of the synovium associated with active inflammatory synovitis. Similar findings are noted on immediate postinjection "blood-pool" images obtained with ^{99m}Tc-MDP, whereas the delayed images show the tracer predominantly localized in the periarticular bone. Gallium-67 is found in all the structures surrounding the affected joints, but it is predominantly localized in the inflamed synovium. This pattern of distribution with gallium is most easily seen in large joints, such as the knee, where capsular uptake will be noted.

In the acute stages of synovitis, the main cellular component of the inflammatory response is the polymorphonuclear leukocyte and, therefore, increased uptake (again, chiefly synovial), rather than decreased uptake of ^{111}In-leukocytes, is to be expected. As the process becomes chronic, lymphocytes appear in greater numbers and the frequency of increased uptake diminishes.

The increased local blood flow associated with synovitis causes an accelerated washout of ^{133}Xe after its instillation into the joint cavity.

(continued on page 2077)